

Supporting Information

Synthesis and characterization of Ag-delfossites AgBO_2 (B: Al, Ga, In) from rapid hydrothermal process

Leon Zwiener^[a], Travis Jones^[a], Elisabeth Hannah Wolf^[a], Frank Girgsdies^[a], Milivoj Plodinec^[a,b], Alexander Yu Klyushin^[a], Elena Willinger^[a], Frank Rosowski^[c,d], Robert Schlögl^[a,e] and Elias Frei^{*[a]}

a] Dr. L. Zwiener, Dr. T. Jones, E. H. Wolf, Dr. F. Girgsdies, Dr. M. Plodinec, Dr. A. Y. Klyushin, Dr. E. Willinger, Prof. Dr. R. Schlögl, Dr. E. Frei
Department of Inorganic Chemistry, Fritz-Haber-Institut der Max-Planck-Gesellschaft, Faradayweg 4-6, 4195 Berlin, (Germany).

E-mail: efrei@fhi-berlin.mpg.de

[b] Dr. M. Plodinec

Division of Material Physics, Boskovic Institute, Bijenička cesta 54, 10000 Zagreb (Croatia).

[c] Dr. A. Y. Klyushin

Division of Energy Material, Helmholtz-Zentrum Berlin für Materialien und Energie GmbH, Albert-Einstein-Str. 15, 12489 Berlin (Germany).

[d] Dr. F. Rosowski

BasCat – UniCat BASF Joint Lab, Technische Universität Berlin, Hardenbergstraße 36, 10623 Berlin (Germany).

[e] Dr. F. Rosowski, Process Research and Chemical Engineering, Process Catalysis Research
BASF SE, Ludwigshafen (Germany).

[f] Prof. Dr. R. Schlögl, Department of Heterogeneous Reactions, Max-Planck-Institut für Chemische Energiekonversion Stiftstrasse 34 – 36, Mülheim an der Ruhr, 45470 (Germany).

Table of contents

S1 Sample overview	3
S2 Synthesis of Ag delafossites	4
S2.1 3R-AgAlO ₂	4
S2.2 3R-AgGaO ₂	9
S2.3 3R-AgInO ₂	10
S3 Characterization	10
S3.1 TEM analysis	10
S3.2 XPS analysis.....	11
S3.3 DRS.....	11
S3.4 Conductivity.....	12
S3.2 Thermal reactivity of 3R-AgBO ₂	13

S1 Sample overview

All samples prepared in this work are listed in the Table S1 – S3.

Table S1: Denomination of samples according to the investigated synthesis parameter. The internal sample identification numbers (ID_{FHI}) are given. Selected samples are part of several series (italic letters) or obtained applying the optimized reaction conditions (bold letters).

B: Al		B: Ga		B: In				
Sample	ID_{FHI}		Sample	ID_{FHI}		Sample	ID_{FHI}	
	As prepared	After STA		As prepared	After STA		As prepared	After STA
Al_1eq	#29179		Ga_1eq	#27430		In_1eq	#27601	
Al_2eq	#29180		Ga_2eq	#27429		In_1.5eq	#27602	
Al_3eq	#29181		Ga_3eq	#27428		In_2eq	#27483	
Al_0.1M	#23236		Ga_30h	#27429		In_1.4g		
Al_0.9M	#29180		Ga_20h	#27439		3R-AgInO₂	#27626	#29288
Al_1.5M	#23660		Ga_10h		#29284			
Al_60h	#29180		3RAgGaO₂	#27445				
Al_45h	#29192							
Al_30h	#25158, #25552	#29286						
3R-AgAlO₂	(IR/Raman)							

Table S2: Hydrothermal synthesis time variation (t). Samples and internal sample identification numbers (ID_{FHI}) are given.

t [h]	ID_{FHI}	t [h]	ID_{FHI}
60	#29179	14	#27430
40	#29180	12	#27429
19	#29181	10	#27428
17	#23236	5	#27429
16	#29180	3	#27439
15.3	#23660		

Table S3: internal sample identification numbers (ID_{FHI}) of 3R-AgAlO₂ scale-up sample.

Sample	ID_{FHI}
Scale-up	#27437

S2 Synthesis of Ag delafossites

S2.1 3R-AgAlO₂

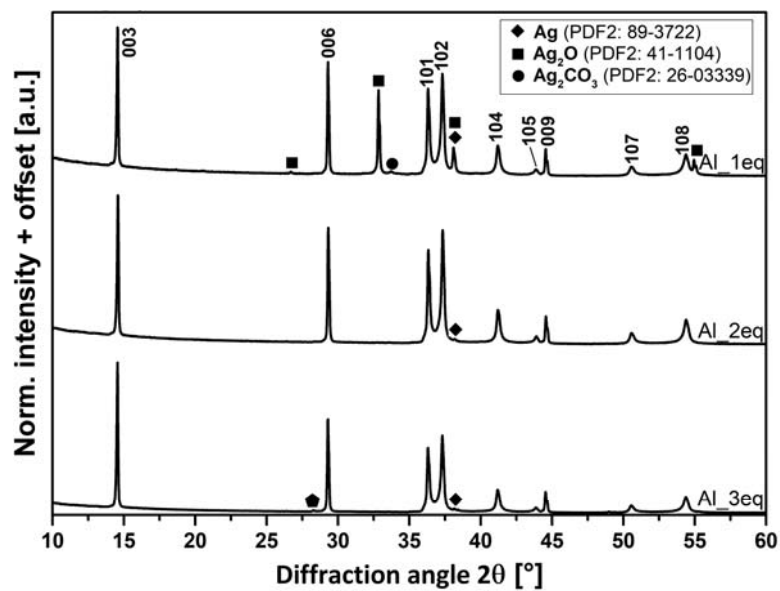


Figure S1: Powder XRD patterns of samples obtained by variation of educt ratios. Reflections of 3R-AgAlO₂ indexed.

Table S4: ICP-OES results of the after-reaction analysis of the colorless liquors of Al_1eq – Al_3eq.

Sample	ICP-OES analysis [mg l ⁻¹]	
	Ag	Al
Al_1eq	15.43	4469
Al_2eq	9.608	7461
Al_3eq	8.502	8503

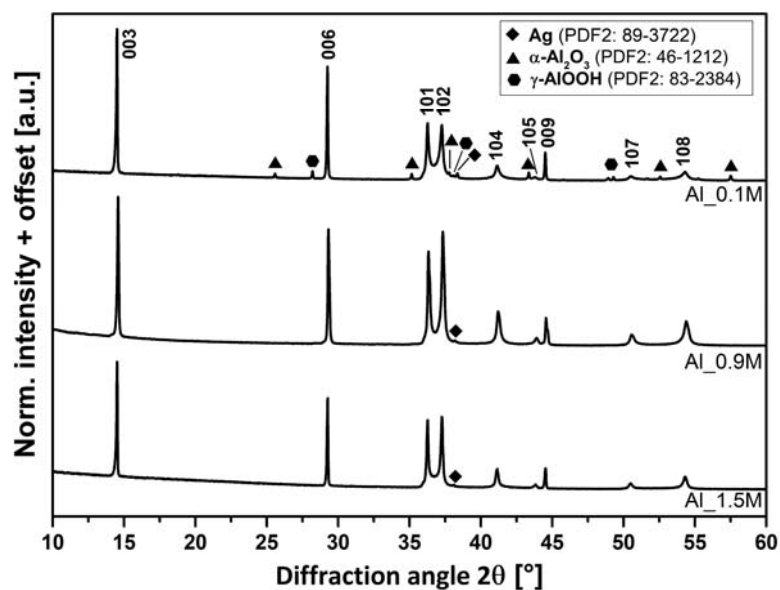


Figure S2: Powder XRD patterns of samples obtained by variation of NaOH concentration. Diffraction peaks of 3R-AgAlO₂ indexed.

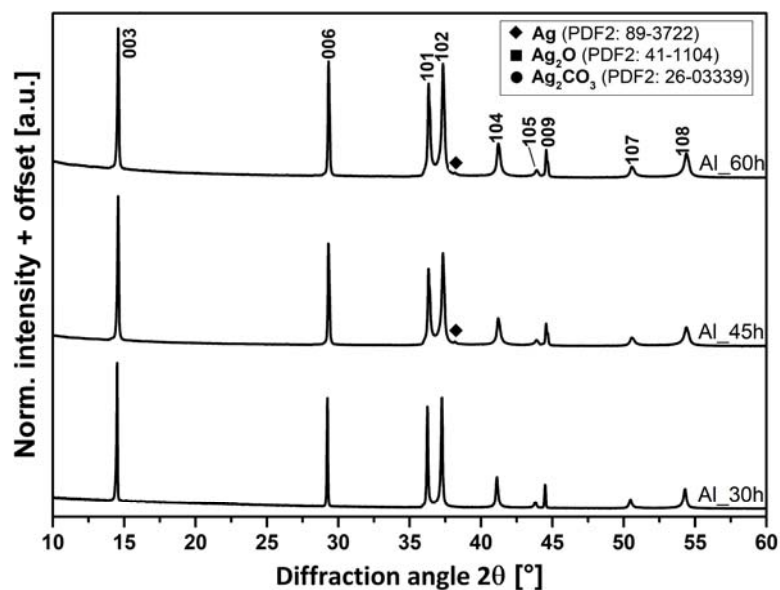


Figure S3: Powder XRD patterns of samples obtained by variation of the hydrothermal synthesis time. Reflections of crystallite main phase 3R-AgAlO₂ indexed.

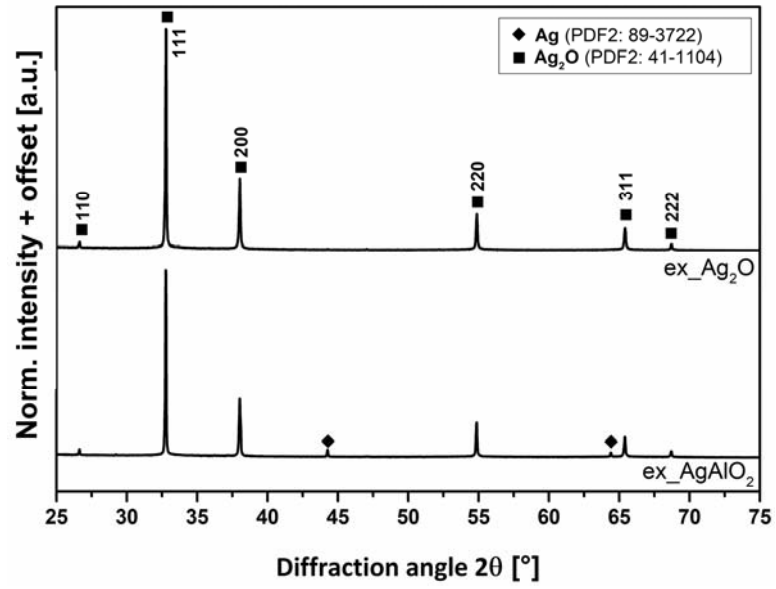


Figure S4: Powder XRD patterns of hydrothermally treated Ag₂O and 3R-AgAlO₂. Reflections of Ag₂O indexed.

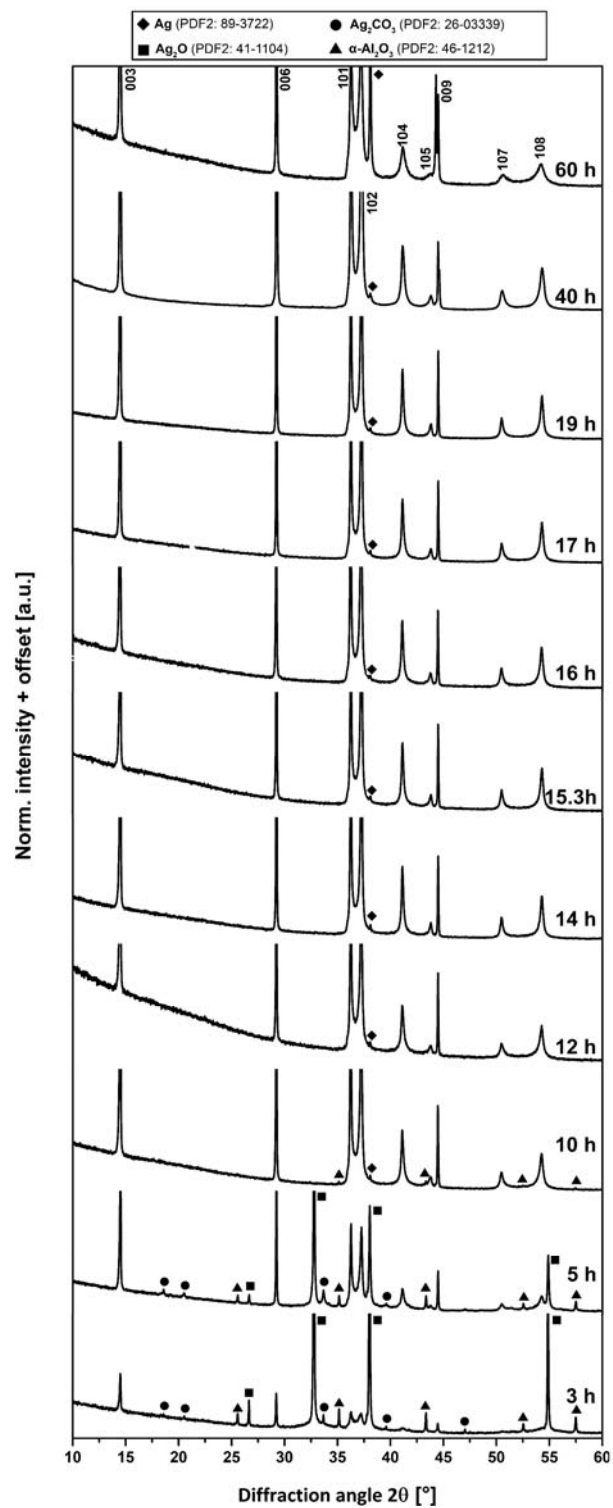


Figure S5: Powder XRD patterns of samples obtained by varying the reaction time from 60 h to 3h. 3R-AgAlO₂ reflections indexed.

For the hydrothermal synthesis a custom-made pressure reactor setup (Picoclave, Büchi) equipped with a 190 ml PTFE lined stainless steel pressure vessel was used. In a typical synthesis Ag_2O (4.043 g, 17.45 mmol, 1.0 eq, >99% Carl Roth) and $\alpha\text{-Al}_2\text{O}_3$ (3.557 g, 34.89 mmol, 2.0 eq, 99+ %, 40 nm APS, Chempur) were mixed in an agate mortar and placed in the PTFE lined pressure vessel, which was then backfilled with NaOH solution (110 ml, 0.9 M, NaOH: >99 %, Carl Roth). The pressure vessel was sealed, and the PTFE stirrer was set up to 250 rpm. The reaction vessel was then heated to the desired reaction temperature of 483 K with a rate of 1.0 Kmin^{-1} . The maximum temperature was held constant for 3 h to 60 h. Pressurized air was used for a controlled cooling back to room temperature in > 90 min. After reaching room temperature, the polycrystalline product was recovered, washed and dried.

An increased amount of 3R-AgAlO_2 was prepared by another 1.5-fold increase of sample size using a custom-made pressure reactor setup (Premex) equipped with a 300 ml PTFE lined Hastelloy C-22 pressure vessel, stirrer and additional top-heating.

The presence of Ag trace amounts (< 1 wt.-%) is evidenced by PXRD analysis for the non-optimized reaction conditions (14h, Scale-Up). Either further parameter adaptation or post-synthesis purification by diluted HNO_3 - treatment (5 M, 45 min) are necessary to obtain phase-pure 3R-AgAlO_2 .

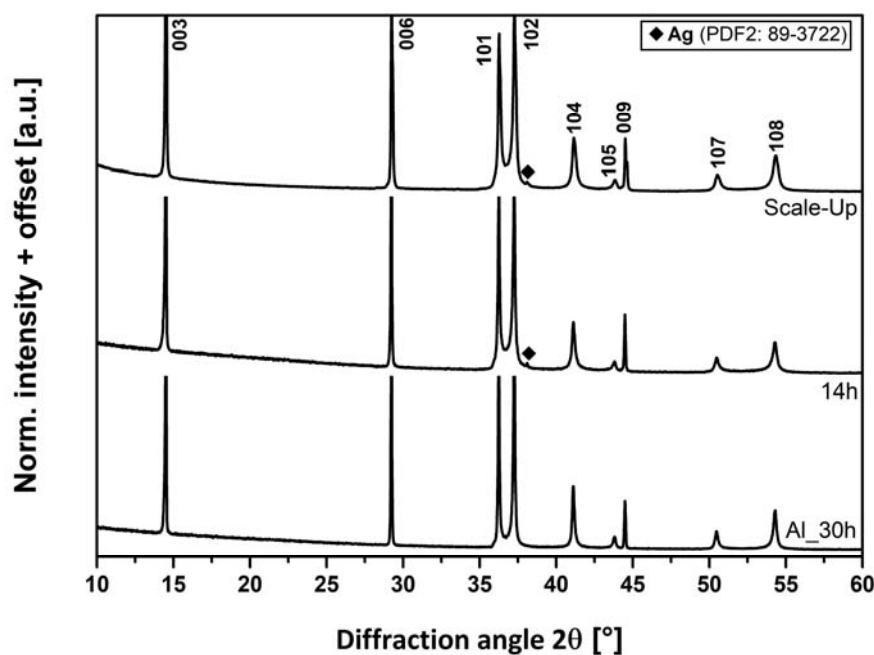


Figure S6: Close ups of PXRD data of $\text{Al}_{30\text{h}}$ (3R-AgAlO_2), 14h (agitation) and scale-up synthesis. Reflections of 3R-AgAlO_2 indexed.

S2.2 3R-AgGaO₂

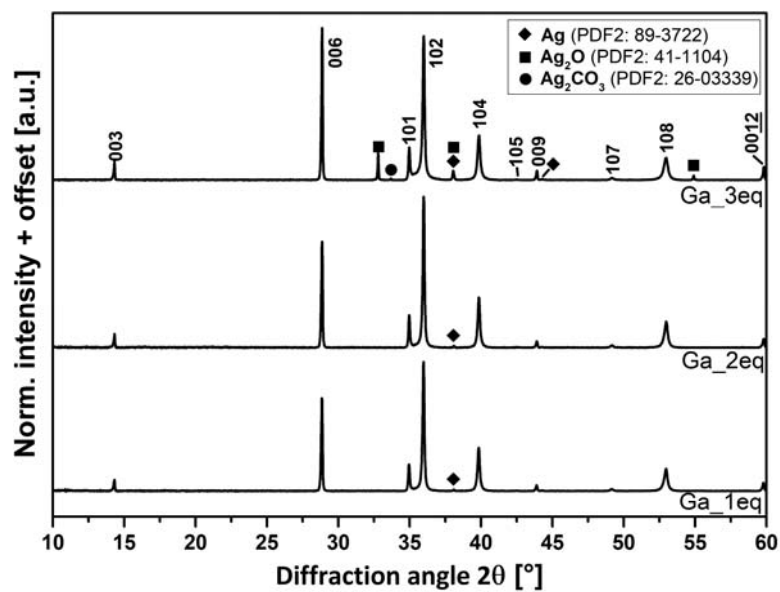


Figure S7: Powder XRD patterns of samples obtained by variation of educt ratios. Reflections of 3R-AgGaO₂ indexed.

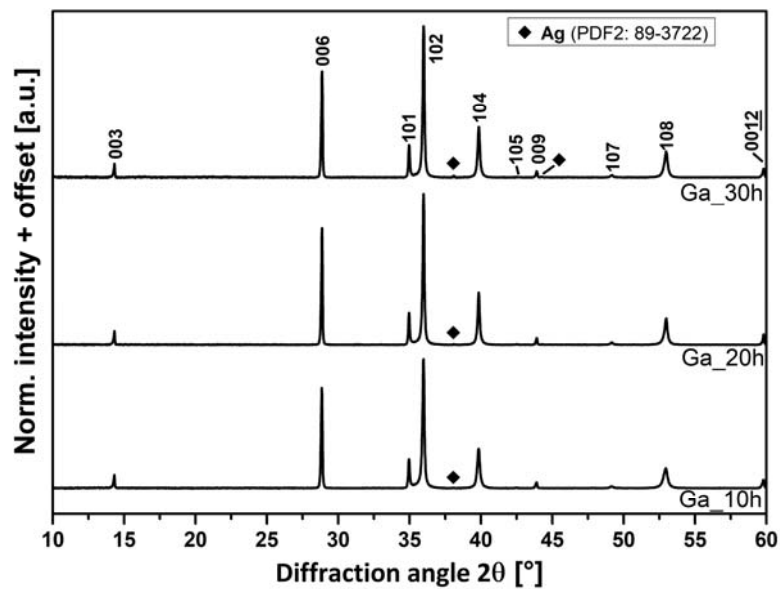


Figure S8: Powder XRD patterns of samples obtained by variation of the hydrothermal synthesis time. Diffraction peaks of 3R-AgGaO₂ indexed.

S2.3 3R-AgInO₂

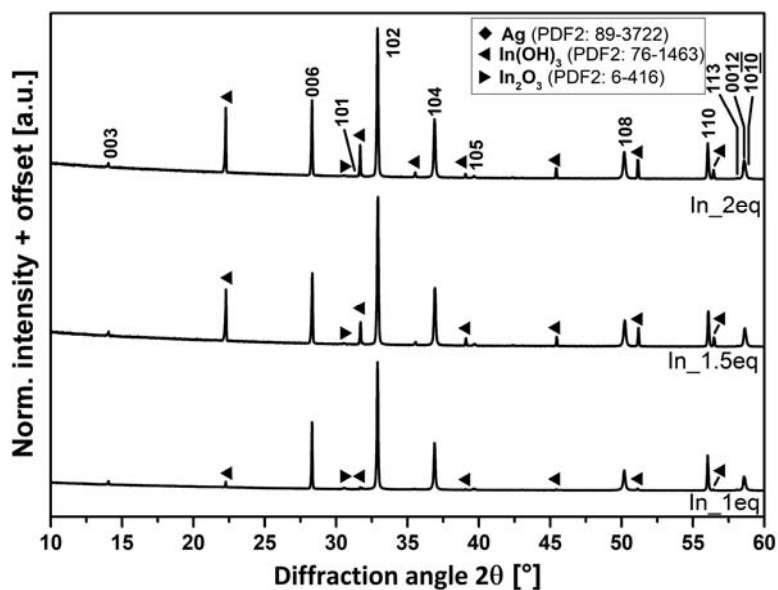


Figure S9: Powder XRD patterns of as-prepared samples obtained by variation of educt ratio. Diffraction peaks of 3R-AgInO₂ indexed.

S3 Characterization

S3.1 TEM analysis

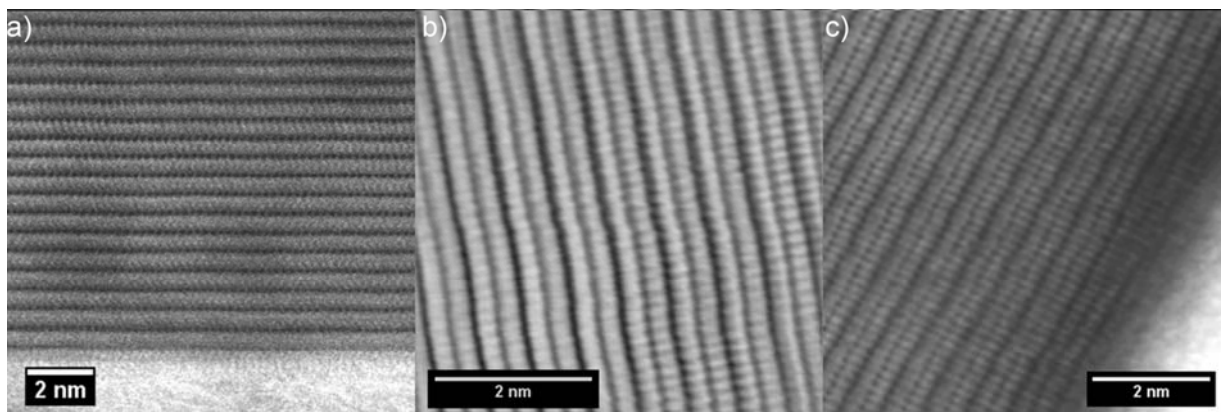


Figure S10: Atomic resolution ABF images of the layered crystalline delafossite structures of a) 3R-AgAlO₂ along the [010] zone axis, b) 3R-AgGaO₂ along the [120] zone axis and c) 3R-AgInO₂ along the [120] zone axis.

S3.2 XPS analysis

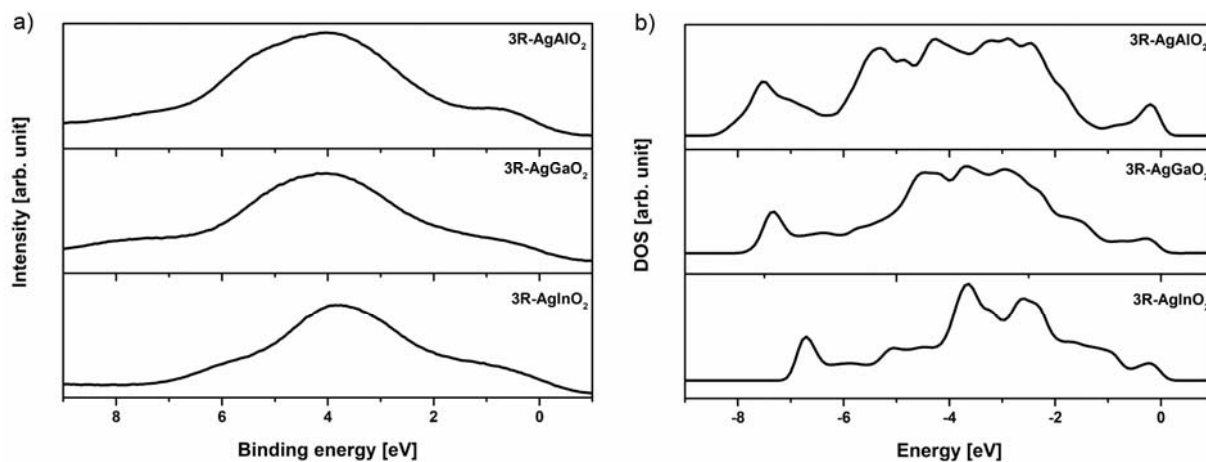


Figure S11: XPS valence band spectra (a) and calculated total DOS (b) of 3R-AgAlO₂ (top), 3R-AgGaO₂ (middle) and 3R-AgInO₂ (bottom panel).

S3.3 DRS

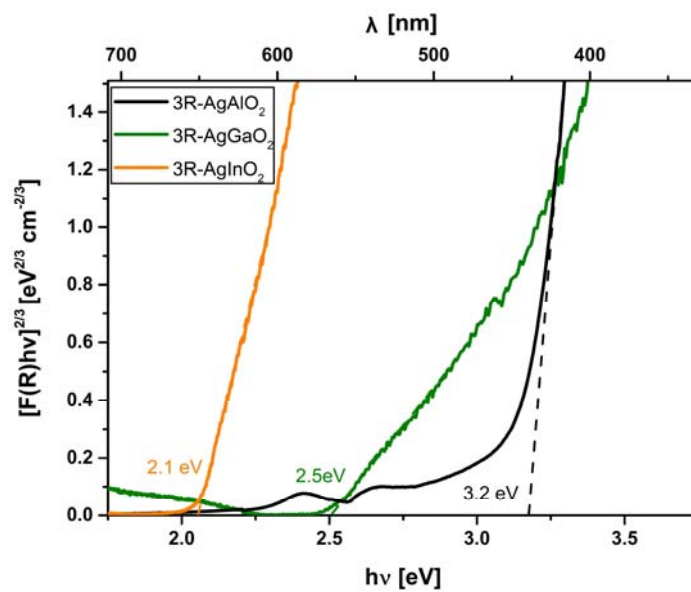


Figure S12: Estimated band gaps from the Tauc plots of 3R-AgBO₂ (B: Al, Ga, In).

S3.4 Conductivity

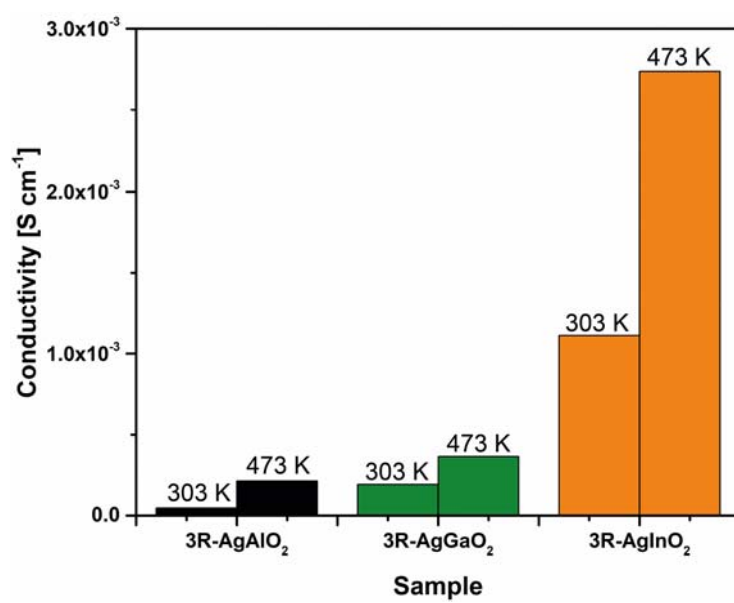


Figure S13: Conductivity of 3R-AgBO₂ (B: Al, Ga, In) as a function of temperature.

S3.2 Thermal reactivity of 3R-AgBO₂

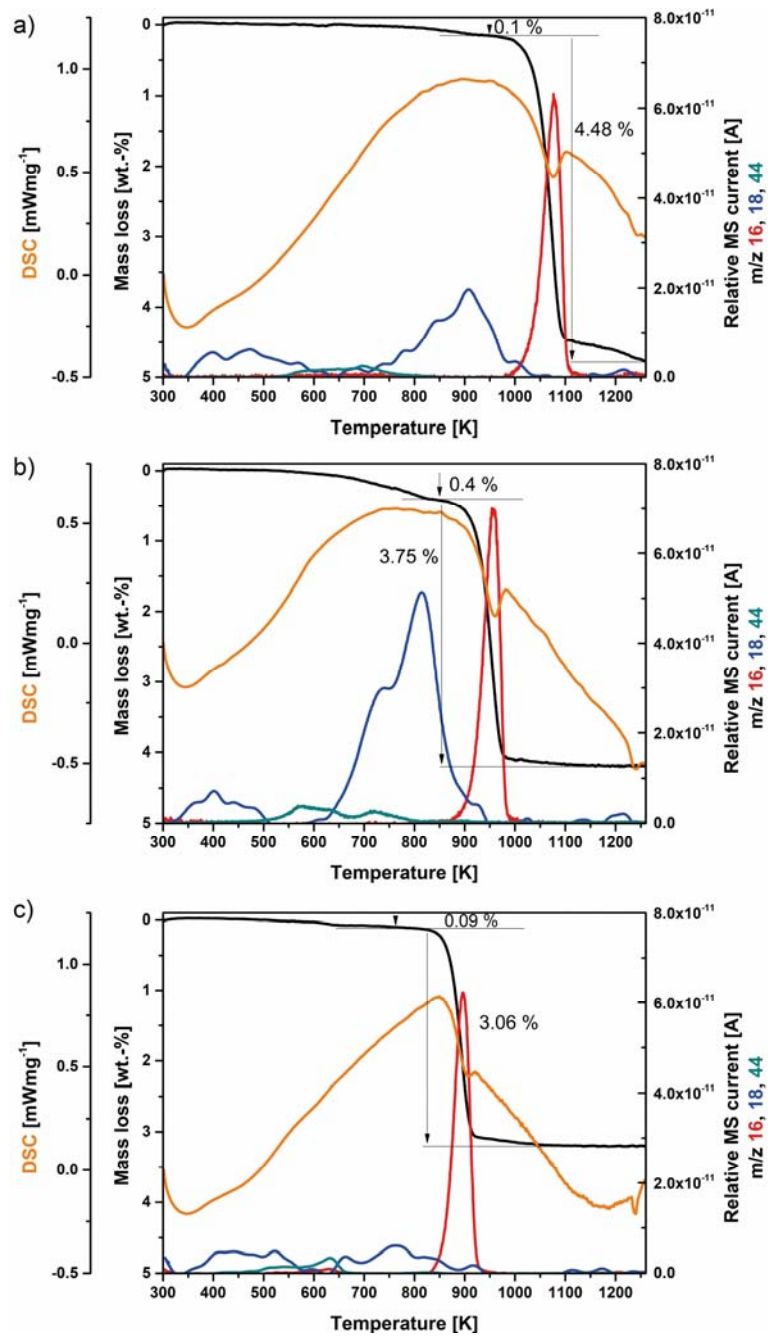


Figure S14: STA/EGA results are given for 3R-AgAlO₂ (a), 3R-AgGaO₂ (b) and 3R-AgInO₂ (c). Mass loss (black line), DSC curve (orange line) and mass spectrometer signal of O (m/z 16, red curve), H₂O (m/z 18, blue curve) and CO₂ (m/z 44, dark cyan curve) are given. STA data (NETZSCH Proteus Thermal Analysis software package, V. 6.10) and EGA data smoothed. The intense O₂ signal (m/z 32) is not shown, due to graphical reason.

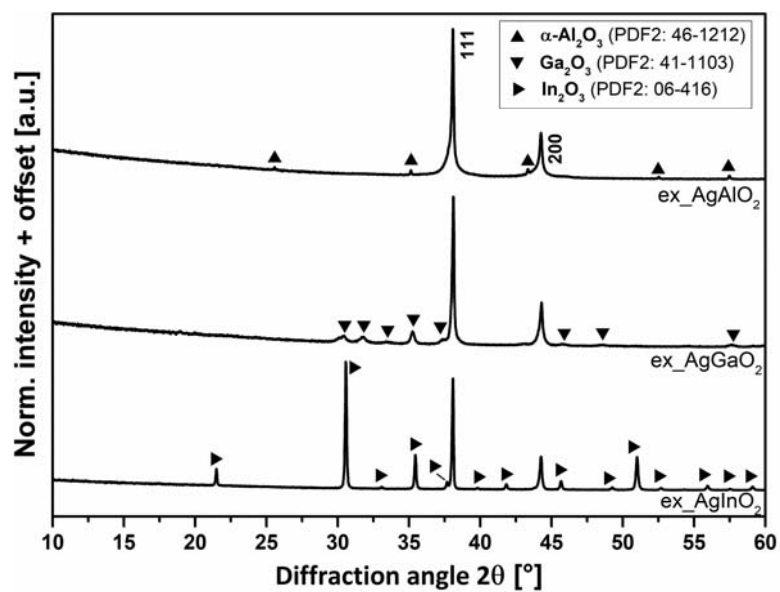


Figure S15: Powder XRD patterns of samples after STA-EGA investigations. Diffraction peaks of Ag (PDF2: 89-3722) indexed.

Temperature-programmed oxidation (TPO) was performed in a fixed-bed quartz reactor using up to 1.5 g 3R-AgBO₂ (*B*: Al, Ga, In). Prior to the experiment, the sample was pre-treated at 873 K (*B*: Al), 823 K (*B*: Ga) or 773 K (*B*: In) for 60 min in He (100 mlmin⁻¹, heating rate 5 Kmin⁻¹). The selected temperatures ensured the integrity of the samples preventing their unintended decomposition (which would lead to the release of oxygen). The sample was cooled back to 300 K in He (100 mlmin⁻¹). The TPO measurement was performed in 0.25 % O₂/He (100 mlmin⁻¹), by applying the same heating rate and dwell time as in the pretreatment. During the experiment, the oxygen consumption was monitored with a paramagnetic detector.

TPO results for 3R-AgAlO₂ are given in Figure S16. No O₂ uptake could be detected in the experiment.

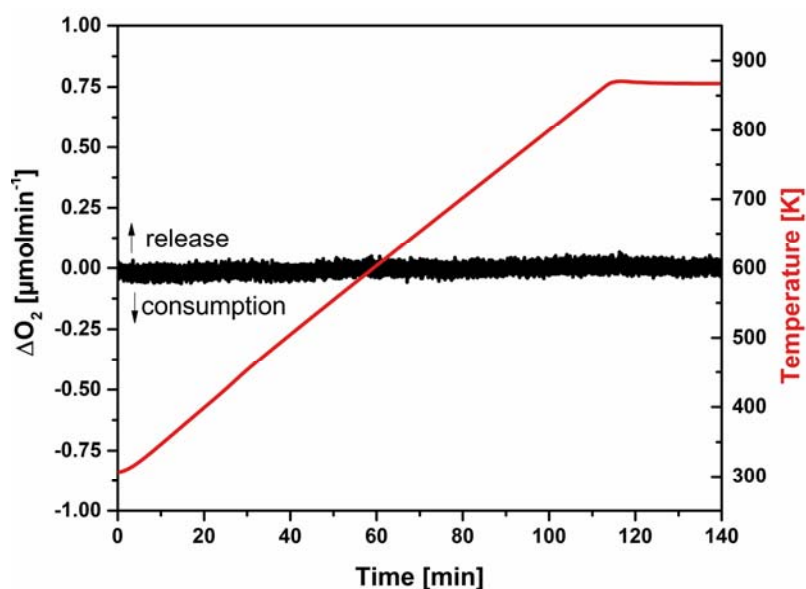


Figure S16: Evolution of the O₂ consumption (-)/evolution (+) rate as a function of the temperature during TPO of 3R-AgAlO₂ in 0.25 % O₂/He.